

Research article

## Bioremediation strategies for hexavalent chromium: Development and safety assessment of recombinant *Escherichia coli* strain 3458



Yeting Weng<sup>a,1</sup>, Qiuying An<sup>a,1</sup>, Dongbei Guo<sup>a</sup>, Ningjing Gan<sup>a</sup>, Weijie Zeng<sup>a</sup>, Wanting You<sup>a</sup>, Zhangye Ma<sup>a</sup>, Jiayan Qi<sup>a</sup>, Zhiyu Zhang<sup>a</sup>, Lirong Zhang<sup>a</sup>, Mufeng Liang<sup>a</sup>, Hongyuan Zeng<sup>a</sup>, Xiaofen Zhang<sup>a</sup>, Changsong Zhao<sup>b</sup>, Ran Zhao<sup>a,\*</sup><sup>1b</sup>

<sup>a</sup> State Key Laboratory of Vaccines for Infectious Diseases, Xiang An Biomedicine Laboratory, National Innovation Platform for Industry-Education Integration in Vaccine Research, School of Public Health, Xiamen University, No. 4221-117 South Xiang'an Road, Xiang'an District, Xiamen, 361102, Fujian, People's Republic of China

<sup>b</sup> School of Public Health, Chengdu Medical College, No. 783 Xindu Avenue, Xindu Street, Xindu District, Chengdu, 610500, Sichuan, People's Republic of China

### ARTICLE INFO

**Keywords:**

Bioremediation  
Hexavalent chromium  
Recombinant strain  
Ecological safety assessment  
Biosafety assessment

### ABSTRACT

Incidents of periodic water pollution and damage to aquatic organisms resulting from the mismanagement of hexavalent chromium emissions have been documented. Utilizing environmentally friendly bioremediation strategies has effectively controlled chromium pollution. The *ChrA* gene, responsible for hexavalent chromium remediation and sourced from *Sporesarcina saremensis* M52, was introduced into *Escherichia coli* to develop recombinant strain 3458. To improve scalability, response surface methodology was used to assess environmental factors influencing recombinant strain 3458's performance, alongside, a safety evaluation examining its impact on aquatic organisms and animals. The study revealed that recombinant strain 3458 possesses adsorption, reduction, and resistance capabilities, which facilitated the transformation of highly toxic hexavalent chromium into the less harmful trivalent form. Nevertheless, the strain may impact *Chlorella* sp., silt communities, and murine liver function through competitive inhibition and endotoxins produced by host cells. These findings offer a comprehensive approach to engineered microbial remediation and provide valuable insights into the safety and effectiveness of this biotechnological solution.

### 1. Introduction

Studies have shown that effluents containing hexavalent chromium [Cr(VI)] are widespread in both industrialized and developing nations, including China, India, the United States, Italy, and Mexico (Chrysochoou et al., 2016; Qiu et al., 2024; Yang et al., 2024). Because of its high solubility in water (Zhao et al., 2023), along with mutagenic, carcinogenic, and teratogenic properties (Layek et al., 2023), Cr(VI) can bioaccumulate and biomagnify within the food chain (Shahid et al., 2017; Xia et al., 2019). This situation presents considerable threats to both ecological equilibrium and human well-being. Conversely, trivalent chromium [Cr(III)] is only one-hundredth as toxic as Cr(VI) and can be more easily precipitated for recovery (Boussouga et al., 2023; Xia et al., 2019). Therefore, the transformation of Cr(VI) to Cr(III) has become the leading approach for treating Cr(VI)-laden effluents (Lei et al., 2023). Bioremediation leverages the metabolic processes of

microorganisms to remove, degrade, or immobilize pollutants. It has emerged as an effective natural solution to heavy metal contamination (González-González et al., 2022; Hou et al., 2020; Qurbani et al., 2022). This method offers several benefits over conventional physical and chemical techniques, including in situ remediation, reduced costs, and minimal secondary pollution (Bharagava and Mishra, 2018; Ly et al., 2024).

Numerous bacterial strains capable of chromium (Cr) removal have been identified (Ahmed, 2014), such as *Bacillus* sp. CRB-B1 (Tan et al., 2020), *Pseudomonas aeruginosa* G12 (An et al., 2020), and *Staphylococcus aureus* K1 (Ahmad et al., 2022). Nonetheless, wild-type strains generally depend on a single pathway of reduction or adsorption for Cr(VI) removal, which restricts their removal efficiency (Thatoi et al., 2014). The inherent advantages of bacterial components, like plasmids, have led researchers to develop genetically engineered microbes for remediation purposes. By modulating metabolic pathways, introducing

\* Corresponding author.

E-mail address: [zhaoran@xmu.edu.cn](mailto:zhaoran@xmu.edu.cn) (R. Zhao).

<sup>1</sup> These authors contributed equally to this work.

additional functional genes, and modifying enzyme affinity and specificity, recombinant DNA technology can enable the creation of enhanced multifunctional strains to significantly improve heavy metal remediation (Raturi et al., 2023).

Previous studies have established that *Sporosarcina saremensis* M52 (M52) exhibits substantial resistance and removal capacity for Cr(VI) (Zhao et al., 2016). Genomic analyses have identified *ChrA* as pivotal in this process (Li et al., 2021). *Escherichia coli* (*E. coli*) stands out as the most advanced host-receptor system in genetic engineering (Ke et al., 2018), providing benefits such as environmental adaptability and operational simplicity (An et al., 2022; Metcalfe et al., 2022). Gabr et al. (2009) also demonstrated that *E. coli* can adsorb Cr(VI). Therefore, engineering an *E. coli* strain to express *ChrA* not only maintains the wild-type strain's high tolerance and Cr(VI) removal efficiency but also improves its environmental adaptability. Additionally, its ease of preparation, low cost, and effective preventability and eliminability highlight its strong application potential (An et al., 2022; You et al., 2024).

Currently, microbial remediation of Cr(VI) primarily involves isolating, screening, and identifying strains capable of Cr(VI) removal (Ayub et al., 2025; Chang et al., 2019; Liu et al., 2019), as well as identifying and validating the associated functional genes (Gu et al., 2020; Li et al., 2025; Stewart et al., 2024). However, there remains a notable deficiency in safety evaluations for these Cr(VI)-removing strains. Notably, certain wild-type Cr(VI)-removing strains may also be pathogenic (Bhunia et al., 2022). Furthermore, the limited understanding of gene functions and expression mechanisms raises concerns about potential ecological impacts (Aryal, 2024; Huang et al., 2024), even when stringent measures are implemented to achieve desirable outcomes. These uncertainties present environmental and health risks, thereby restricting the use of microbial remediation techniques (Maqsood et al., 2023; Xiao et al., 2023). Consequently, a biosafety assessment is legally mandated before utilizing such microorganisms for sewage treatment (Glandorf, 2019).

In this study, we engineered a recombinant *E. coli* strain (3458) expressing *ChrA*, investigated mechanism and demonstrated its superior chromium removal ability and environmental adaptability compared to the wild strain M52. The objective was to develop a highly resistant and adaptable strain possessing both adsorption and reduction capabilities to enhance effectiveness in complex Cr(VI) remediation settings. Furthermore, when the recombinant strain 3458 was introduced into Cr(VI)-containing wastewater, the removal of Cr(VI) resulted in the formation of a complex reduction system (RS) (Li et al., 2021). Therefore, the safety of the RS is assessed alongside the strain, providing valuable insights into the strain's applicability for real-world scenarios and contributing to a comprehensive framework for the future deployment of recombinant strains in mitigating environmental Cr(VI) contamination.

## 2. Materials and methods

### 2.1. Construction and validation of the recombinant strain

Primers *ChrA*-F and *ChrA*-R were designed and synthesized based on the M52 gene sequence (Table S1). The *ChrA* gene was polymerase chain reaction (PCR)-amplified from M52 genomic DNA (Tables S2 and S3). The pET-28a(+) expression vector and the purified PCR product were digested with *BamH* I and *Hind* III, ligated, and transformed into *E. coli* Trans5a competent cells. Transformed pET-28a(+)–*ChrA*/*E. coli* Trans5a was selectively cultured on Luria–Bertani (LB) agar supplemented with kanamycin. Plasmid purification of pET-28a(+)–*ChrA* was performed using a Plasmid Extraction Kit (TIANGEN, Beijing, China), and the recombinant plasmid was subsequently transformed into *E. coli* BL21 (DE3).

Recombinant pET-28a(+)–*ChrA* was verified via double enzyme digestion and sequencing. A colony of recombinant strain 3458 was inoculated into LB broth containing 50 µg mL<sup>-1</sup> kanamycin and

incubated at 37 °C until reaching the logarithmic phase, after which 1 mM isopropyl-β-D-thiogalactoside (IPTG) was added to induce recombinant protein expression. Expression samples at 0, 2, 4, 6, 8, and 10 h were extracted and analyzed by sodium dodecyl sulfate–polyacrylamide gel electrophoresis (SDS-PAGE) (Mertes et al., 2024; Zhang et al., 2021). Following induction of protein expression, intracellular soluble fractions and inclusion bodies were isolated for SDS-PAGE analysis to determine the localization and assess the solubility of the recombinant protein.

### 2.2. Cr(VI) resistance and removal ability

Additionally, a single colony of strain 3458 was inoculated into 100 mL of LB liquid medium for shaking culture (37 °C, 200 rpm) until the optical density at 600 nm (A<sub>600</sub>) reached 0.6–0.7 to obtain the seed culture. The seed culture was then inoculated at 4 % of the inoculum into an LB medium containing Cr(VI) (0, 50, 100, 200, 300, 400, 500, 600, 700, and 800 mg L<sup>-1</sup>) and incubated at pH 8.0 and 37 °C. Aliquots were sampled at 0, 12, 24, 36, 48, 60, and 72 h, and A<sub>600</sub> was measured to evaluate growth and resistance to Cr(VI). The Cr(VI) content in the culture medium was quantified using dibenzoyldihydrazine spectrophotometry (An et al., 2022) to assess the removal capacity of the recombinant strain.

### 2.3. Factors influencing Cr(VI) removal

To determine the influence of environmental factors and establish optimal conditions for recombinant strain 3458, thirty combinations of pH (6.5, 7.0, 7.5, 8.0, 8.5, and 9.0) and incubation temperature (25, 30, 35, 40, and 45 °C) were analyzed using response surface methodology (Rincon et al., 2024). Four treatment groups (Cu(II), Fe(II), Mn(II), and SDS) were created to investigate the impacts of metal ions and small molecules. All groups were incubated for 48 h at 200 rpm and 37 °C, with Cr(VI) content measured every 12 h using dibenzoyldihydrazine spectrophotometry.

### 2.4. Characterization of Cr(VI) removal

The seed solution was inoculated into an LB liquid medium containing 100 mg L<sup>-1</sup> Cr(VI) and a Cr(VI)-free control medium. After 48 h of incubation, cells were harvested by centrifugation and rinsed with phosphate-buffered saline (PBS). The samples were fixed as described elsewhere (Long et al., 2013). Cell surface morphology was examined using scanning electron microscopy (SEM) combined with energy dispersive spectrometry (EDS) at an accelerating voltage to determine the energy of photons in the X-ray spectrum as they interact with material elements on the cell surface (Harutyunyan, 2022). X-ray diffraction analysis (XRD) characterized the Cr crystals by comparing the diffraction patterns of control and Cr(VI)-treated cultures (Pandey et al., 2021). Fourier transform infrared spectroscopy (FT-IR) assessed various functional clusters and potential sites involved in Cr(VI) adsorption or removal on the cell surface (Berna, 2017). X-ray photoelectron spectroscopy (XPS) analyzed the chemical composition of the cell strain (Krishna and Philip, 2022). FT-IR, XPS, and XRD analyses were performed at the SL Intelligent Analysis Testing Center (Nanjing, China).

### 2.5. Ecological safety evaluation of recombinant strain 3458 and its reduction system

#### 2.5.1. Biological community experiment of sludge in water bodies

Silt samples were collected from the Xi River near Binhai West Avenue, Tong'an District, Xiamen, China (24.64°N, 118.15°E) at a depth of 15 cm and stored at –20 °C. Centrifuge tubes served as culture vessels, and a recombinant strain 3458 reduction system (3458RS) solution containing recombinant strain 3458 and 100 mg L<sup>-1</sup> Cr(VI) was added to the silt culture for 14 d (Table S4). The control settings are listed in Table S4, including a positive control (PC) of 100 mg L<sup>-1</sup> Cr(VI) +

sludge, a negative control (NC) of sterile water + sludge, and a baseline control (BC) group of original sludge matrix, which are used to assess the background effects of the sediment itself. Genomic DNA was extracted from silt samples using the cetyltrimethylammonium bromide method, followed by the addition of specific primers for PCR amplification to characterize microbial diversity. The library was constructed using TruSeq DNA PCR-Free Sample Preparation Kit (Illumina, Beijing, China) and quantified by Qubit and quantitative PCR (Q-PCR). After quality verification, sequencing was performed on the NovaSeq6000 platform. Sequencing data were clustered into Operational Taxonomic Units (OTUs) at 97 % identity, and OTU sequences were annotated with species names. Additionally, OTUs were matched to the FAPROTAX database for functional annotation.

### 2.5.2. Growth inhibition test of *Chlorella* sp

The pET-28a(+) expression vector, containing the functional gene fragment *ChrA* from M52, was transformed into *E. coli* BL21 to create the recombinant strain 3458. With reference to You et al. (2024) and Chen et al. (2025), M52 and pET-28a(+)/*E. coli* BL21 (pET-28a) were also included as controls. Subsequently, the M52, M52 reduction system (MRS), 3458, 3458RS, pET-28a, pET-28a reduction system (pET-28aRS), NC, and PC groups were utilized to assess their effects on *Chlorella* growth (Table S5). Cultures were incubated for 14 d at 23 °C and under 12 h light and 12 h dark cycles, maintaining the same initial concentration. Growth was assessed by measuring  $A_{600}$  every 2 d using a microplate spectrophotometer (Epoch2T, BioTek, U.S.A.). *Chlorella* cell counts were quantified using the blood cell plate method under an upright microscope (Leica DM4B, JINGYIXINGYE, China). The concentration of *Chlorella* cell per mL was determined by multiplying the total cell count in five medium squares by  $5 \times 10^4$ .

### 2.6. Biosafety evaluation of recombinant strain 3458 and its reduction system

#### 2.6.1. Acute toxicity test in mice

Forty male ICR mice (18–22 g) were obtained from the Xiamen University Animal Center. All animal procedures were approved by the Xiamen University Institutional Animal Care and Use Committee (Ethics code: XMULAC20200002). Mice were fed according to the National Research Council's Guide for the Care and Use of Laboratory Animals for one week before the start of the study to acclimatize them to the laboratory environment (Council, 2011). Similar to the *Chlorella* growth inhibition assay, M52, MRS, 3458, 3458RS, pET-28a, pET-28aRS, NC, and PC groups were established (Table S6) to assess the strain's safety. The strain was cultured to the stationary phase, centrifuged at 861×g for 15 min at 4 °C, then resuspended in PBS and washed with normal saline. Subsequently, appropriate volumes of normal saline were added to prepare samples containing  $1.0 \times 10^9$  CFU mL<sup>-1</sup> viable bacteria for gavage administration. In this acute oral toxicity study, mice received two gavage doses at 2 % of body weight, 12 h apart. Observations were performed for 14 d, and weight was measured every 2 d to record the changes in each group.

#### 2.6.2. Determination of major organ coefficients and serum biochemical indices

On day 15, all mice were fasted for 8 h and weighed, blood samples were collected from the ophthalmic vein before cervical dislocation. All tissues and organs were subjected to a gross pathological examination. The liver, kidneys, and spleen were harvested and their wet weights measured. Organ coefficients were determined using the formula: organ coefficient = (organ wet weight/body weight at sacrifice) × 100 % (Amanat et al., 2023).

Blood samples were placed in anticoagulant centrifuge tubes for 1 h and then centrifuged (9569×g, 10 min, 4 °C) to obtain serum. Serum levels of alanine aminotransferase (ALT), aspartate aminotransferase (AST), alkaline phosphatase (ALP), total bilirubin (T-Bil), total protein

(TP), globulin (GLB), urea, uric acid (UA), total cholesterol (TC), tri-glyceride (TG), high-density lipoprotein cholesterol (HDL-C), low-density lipoprotein cholesterol (LDL-C), magnesium (Mg), calcium (Ca), and phosphorus (P) were quantified using an automated biochemical analyzer and corresponding kits (Mindray, Shenzhen, China).

#### 2.6.3. Analysis of liver tissue sections

The largest lobe of the weighed liver was immersed in 4 % paraformaldehyde, fixed for 24 h, and then cut into pieces and placed in an embedding box for tissue dehydration, paraffin embedding, and sectioning. Tissue sections were mounted on glass slides, stained with hematoxylin and eosin (HE), and histopathological alterations were assessed via microscopy (Leica, Germany). Paraffin-embedded sections were deparaffinized with xylene (10 min, twice), rehydrated sequentially with ethanol (100 % for 5 min, 90 % for 2 min, 70 % for 2 min) and ddH<sub>2</sub>O (2 min), and then processed following the one-step TdT-mediated dUTP nick-end labeling (TUNEL) apoptosis detection kit protocol (Beyotime, Shanghai, China). Post-labeling, the sections were examined under a fluorescence microscope (Leica, Germany) using excitation and emission wavelengths of 450–500 nm and 515–565 nm respectively, to identify apoptotic cells.

#### 2.6.4. Liver oxidative stress indicators and apoptotic protein assays

Liver samples (0.1 g) were rinsed with 10 % PBS, dried, and transferred to 1.5 mL centrifuge tube. Subsequently, 0.9 mL saline and sterile steel beads were added, and the samples were homogenized at 60 Hz for 90 s using a tissue grinder (JingXin, Shanghai, China). All procedures were performed on ice to obtain a 10 % tissue homogenate. Oxidative stress in the tissue homogenate was measured using superoxide dismutase (SOD), glutathione peroxidase (GSH-Px), and malondialdehyde (MDA) kits (Jiancheng, Nanjing, China) (Li et al., 2024).

Protein was extracted from liver tissue homogenate, and its concentration was measured using a bicinchoninic acid protein detection kit (Meilunbio, Dalian, China). The protein samples were separated by SDS-PAGE and subsequently transferred to nitrocellulose membranes (10 A, 8 min). The membranes were blocked with 1 % calf serum for 1 h at room temperature, then incubated overnight at 4 °C with primary antibodies targeting tubulin, B-cell lymphoma-2 (Bcl-2), and Bcl-2-associated x (Bax). After washing (1 × Tris-buffered saline with Tween 20, 5 min, 3 times), the membranes were incubated with a goat anti-rabbit immunoglobulin G-conjugated secondary antibody for 1 h at room temperature. The blots were visualized using a chemiluminescence imaging system. Band quantitation was performed with ImageJ software using tubulin as an internal reference, to calculate target protein expression (You et al., 2024).

### 2.7. Statistical analysis

Statistical analyses were conducted using SPSS software. Growth curves of the strains and *Chlorella* were compared with the nonparametric Mann-Whitney test for independent samples. The alpha diversity indices between groups were assessed using t-tests and Wilcoxon tests. Inter-group FAPROTAX analyses were compared using t-tests. Weight change trends were analyzed via repeated measures analysis of variance. Strain growth curves, organ coefficients, blood biochemical indicators, oxidative stress indicators, apoptosis counts, and apoptosis protein content were analyzed using one-way analysis of variance. The obtained values are expressed as mean ± standard deviation ( $\bar{x} \pm s$ ), with statistically significant differences indicated by  $p < 0.05$ .

## 3. Results and discussion

### 3.1. Construction and validation of the recombinant strain

The recombinant plasmid containing *ChrA* was successfully

constructed, as depicted in Fig. S1a. PCR amplification products were confirmed through agarose gel electrophoresis and sequencing analysis. Based on 1.5 % agarose gel electrophoresis, the length of the untreated recombinant plasmid was found to be approximately 6500 bp. Following double digestion, the plasmid was cleaved into fragments of roughly 5300 bp and 1200 bp, with the shorter fragment corresponding to the *ChrA* sequence (1194 bp). Sequencing of the shorter fragment revealed a 99.4 % similarity to the target *ChrA* gene, confirming the successful cloning of *ChrA* into pET-28a(+) .

Protein expression in recombinant strain 3458 was evaluated by SDS-PAGE (Fig. S1b). The protein band at 45 kDa is 2 kDa larger than *ChrA*'s expected size of 42.9 kDa, confirmed the successful expression of *ChrA*. Protein expression remained relatively constant during the initial 4 h. This may be due to factors, such as growth medium composition, induction timing, and the duration of the IPTG induction phase. Moreover, IPTG must enter the cells through LacY active transport or passive diffusion to effectively induce protein expression, a process that does not occur instantaneously (Simas et al., 2023). The *ChrA* protein in recombinant strain 3458 was highly expressed during the detergent stage, as shown in Fig. S1c, and exhibited a molecular weight of approximately 45 kDa. This result aligns with the characterization of *ChrA* as a hydrophobic transmembrane protein within the chromate ion transporter superfamily (Díaz-Pérez et al., 2007), thereby validating the successful construction of recombinant strain 3458 and the effective expression of *ChrA*.

### 3.2. Cr(VI) resistance and removal ability

As illustrated in Fig. S2, the growth curve of strain 3458 remained stable and demonstrated better tolerance than the other two strains within the 0–200 mg L<sup>-1</sup> Cr(VI) range. However, all strains showed slow growth at 400 mg L<sup>-1</sup> and 800 mg L<sup>-1</sup> Cr(VI). All strains completely removed 100 mg L<sup>-1</sup> Cr(VI) within 48 h, with the time required for complete removal increased as Cr(VI) concentration increased. Within the range of 400 mg L<sup>-1</sup> to 800 mg L<sup>-1</sup> Cr(VI), the removal rate was low, corresponding to the growth-inhibitory assay. This observation supports

the hypothesis that, similar to the findings of Karthik et al. in *Cellulosimicrobium funkei* strain AR8 (Karthik et al., 2017), elevated Cr(VI) concentrations adversely affected survival and activity, resulting in diminished removal efficiency.

The results showed that the recombinant strain 3458 possessed a high level of resistance, being able to fully tolerate and effectively remove Cr(VI) concentrations up to 200 mg L<sup>-1</sup>. Therefore, a concentration of 100 mg L<sup>-1</sup> Cr(VI) was selected to further characterize the strain and examine the factors affecting Cr(VI) removal. This selection ensured that the recombinant strain 3458 retained its robust resistance and removal capabilities. Additionally, establishing a 100 mg L<sup>-1</sup> Cr(VI) benchmark is practically significant, aligning with the data we gathered from monitoring Cr(VI) levels in the collection ponds of industrial wastewater treatment facilities.

### 3.3. Effect factors of Cr(VI) removal

Removal efficiency is often influenced by factors such as the temperature, pH, metal ions, and small molecules, which primarily affect the availability of heavy metal ions, reductase activity, and active binding sites on the cell surface (Wu et al., 2019). According to Zhao et al. (Zhao et al., 2016), the optimal temperature and pH for strain M52 are 35 °C and 8.0, respectively. As shown in Fig. 1, the recombinant strain 3458 performed well between 30 and 45 °C and pH 7.0–8.5, with its removal function inhibited solely by SDS, making it more environmentally suitable than M52. The higher pH also reduces Cr(VI) formation in water (Tan and Liu, 2023), and given the superior resistance of strain 3458 in studies concerning Cr(VI) resistance and removal capacity, the recombinant strain 3458 presents greater potential for application and aligns more closely with the demands of real-world remediation conditions.

### 3.4. Characterization of Cr(VI) removal

As depicted in Fig. 2, all strains exhibited a blunt, rod-shaped morphology with smooth surfaces and no adhesion in Cr(VI)-free

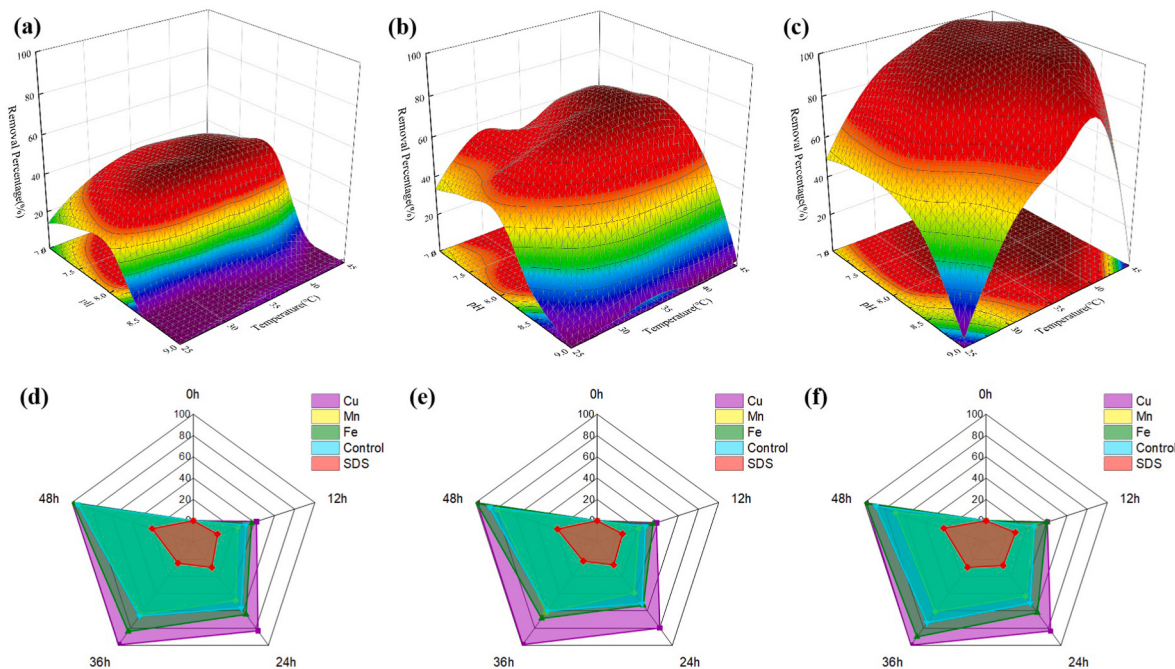


**Fig. 1.** Environmental factors affecting the removal of Cr(VI). Response surface 3D plot of temperature versus pH showing the effect of independent variables on the removal of Cr(VI) by recombinant strain 3458 at (a) 12 h, (b) 24 h and (c) 48 h. The higher the removal rate is, the darker red the color appears; the lower the removal rate is, the darker blue the color appears. Radar chart of metal ions and small molecules showing the effect on the removal of Cr(VI) by (d) strains M52, (e) recombinant strain 3458 and (f) pET-28a. The shaded area is used to indicate the strain's ability to removal Cr(VI).

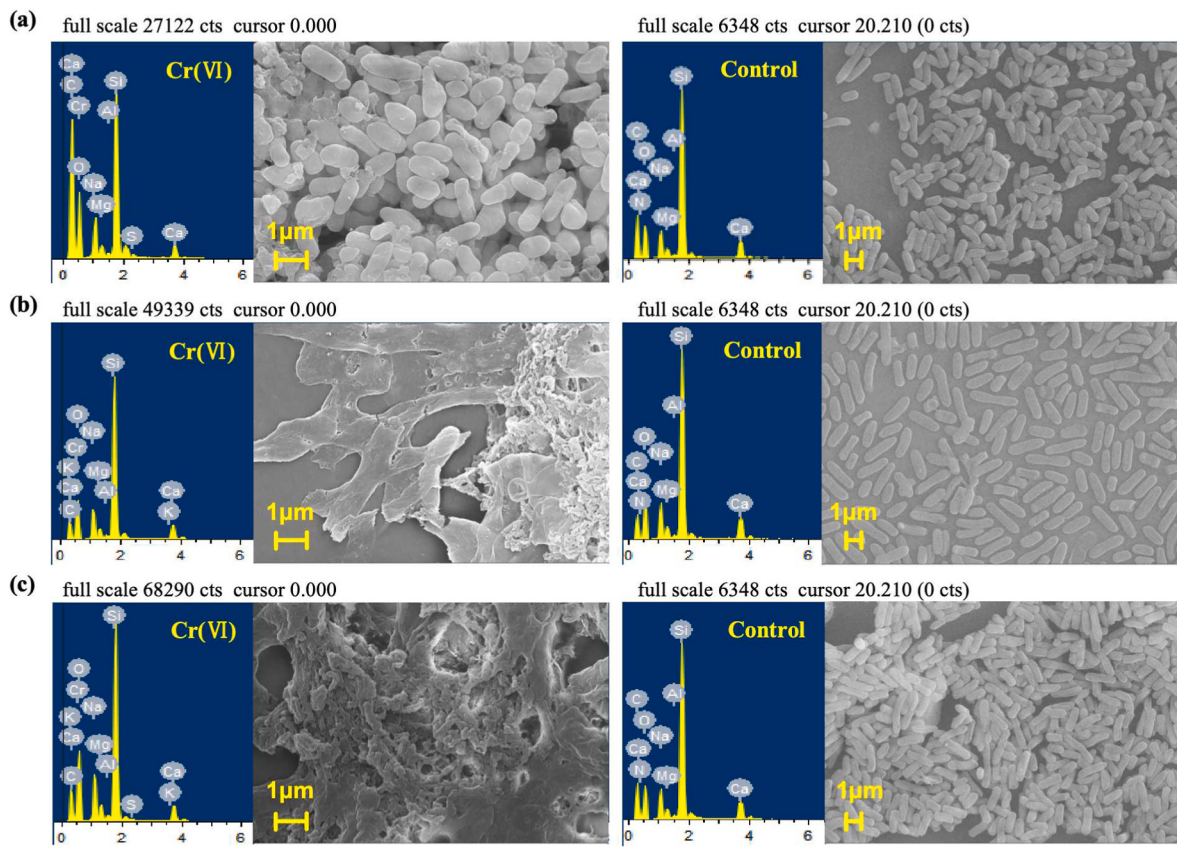


**Fig. 2.** SEM-EDS analysis of (a) M52, (b) recombinant strain 3458 and (c) pET-28a. Strains cultivated on LB medium with and without  $100 \text{ mg L}^{-1}$  Cr(VI) were used as the Cr(VI) group and control group, respectively.

media. In contrast, both pET-28a and recombinant strain 3458 showed varying degrees of adhesion and surface folding, while M52 displayed swelling and rupture in the presence of Cr(VI). As described elsewhere (Samuel et al., 2013), Cr(VI) induced morphological changes in the strains. EDS analysis revealed that Cr was absent on the cell surface of control groups but present on those treated with Cr(VI) (Fig. 2). The Cr content was significantly higher on the surface of recombinant strain 3458 (0.12 %) compared to M52 (0.04 %) and pET-28a (0.04 %), demonstrating that recombinant strain 3458 has a superior Cr adsorption capacity (Fig. S3). However, the valence state of adsorbed Cr on the surface remains undetermined and requires further analysis using XRD, XPS, and FT-IR experiments.

XPS analysis showed that Cr(VI) altered the peaks of C, N, O, Na, and Cr on the surfaces of all strains (Fig. 3a–c). The two weak peaks at 577.50 eV ( $\text{Cr}^{3+} 2\text{p}_{3/2}$ ) and 587.26 eV ( $\text{Cr}^{3+} 2\text{p}_{1/2}$ ) correspond to the Cr(III) characteristic peaks (Qi et al., 2023) (Fig. 3e), demonstrating the ability of recombinant strain 3458 to reduce Cr(VI) to Cr(III) on the cell surface. As shown in Fig. 3d and f, M52 and pET-28a also have characteristic peaks corresponding to Cr(III), indicating that M52, recombinant strain 3458, and pET-28a effectively reduce Cr(VI) to Cr(III). This finding is further corroborated by changes in the XRD diffraction peaks across all strains (Fig. 3g–i).

FT-IR analysis of M52 (Fig. 3j) revealed no significant loss or shift in absorption peaks after Cr(VI) treatment, indicating that M52 primarily mediates Cr(VI) reduction via intracellular enzymatic mechanisms rather than through cell surface adsorption or functional modification, thus supporting previous studies (Li et al., 2021). Upon exposure to  $100 \text{ mg L}^{-1}$  Cr(VI), the peaks of pET-28a at  $1237 \text{ cm}^{-1}$ ,  $1359 \text{ cm}^{-1}$ , and  $1450 \text{ cm}^{-1}$  disappeared (Fig. 3l). Conversely, the intensities of the peaks at  $2845 \text{ cm}^{-1}$ ,  $2925 \text{ cm}^{-1}$ , and  $3057 \text{ cm}^{-1}$  were diminished, suggesting that the reduction and adsorption capabilities of pET-28a may be associated with carboxyl, nitro, and hydroxyl functional groups. Similarly,

for strain 3458 (Fig. 3k), the peaks at  $1088 \text{ cm}^{-1}$  and  $1233 \text{ cm}^{-1}$  vanished, implying that the reduction of Cr(VI) involves the phosphoric acid and carboxyl groups of the cell membrane. The peaks at  $2861 \text{ cm}^{-1}$ ,  $2921 \text{ cm}^{-1}$ , and  $3285 \text{ cm}^{-1}$  were shifted, suggesting that amide and alkyl groups can bind to Cr(VI), again proving the Cr(VI) adsorption capacity of recombinant strain 3458 and the function of *ChrA*.

Pimentel et al. (2002) found that a strain expressing the *ChrA* protein accumulated more Cr(VI) in everted membrane vesicles. Additionally, during the reaction process, Cr(VI) may be adsorbed by specific functional groups on the cell membrane (Tan et al., 2020), with some functional groups, such as hydroxyl groups, linked to Cr(VI) reduction products (Yang et al., 2024). Combining the characterisation results, recombinant strain 3458 can reduce Cr(VI) to Cr(III), with this process mainly occurring on the cell surface. Amides and alkyl groups are involved in the Cr(VI) adsorption, and the *ChrA* protein increases Cr(VI) accumulation on the cell membrane surface. Furthermore, phosphate and carboxyl groups on the cell membrane play crucial roles in the Cr(VI) reduction process. Thus, recombinant strain 3458 effectively removes Cr(VI) mainly through functional groups adsorption and membrane-associated reduction reactions. Mohamed et al. (Mohamed et al., 2020) isolated chromate reductase genes from *E.coli*, suggesting that strain 3458 might also have an intracellular enzymatic mechanism for reducing Cr(VI). However, further research is needed to confirm the presence of an intracellular enzymatic mechanism in the strain. Based on these analyses, we conclude that recombinant strain 3458 possesses greater adsorption and resistance compared to M52 and pET-28a by removing Cr(VI) through the functional groups on the cell surface and adsorbing its reduced products, both of which are favorable for metal recovery. Nonetheless, potential ecological and biological impacts must be explored before practical application.

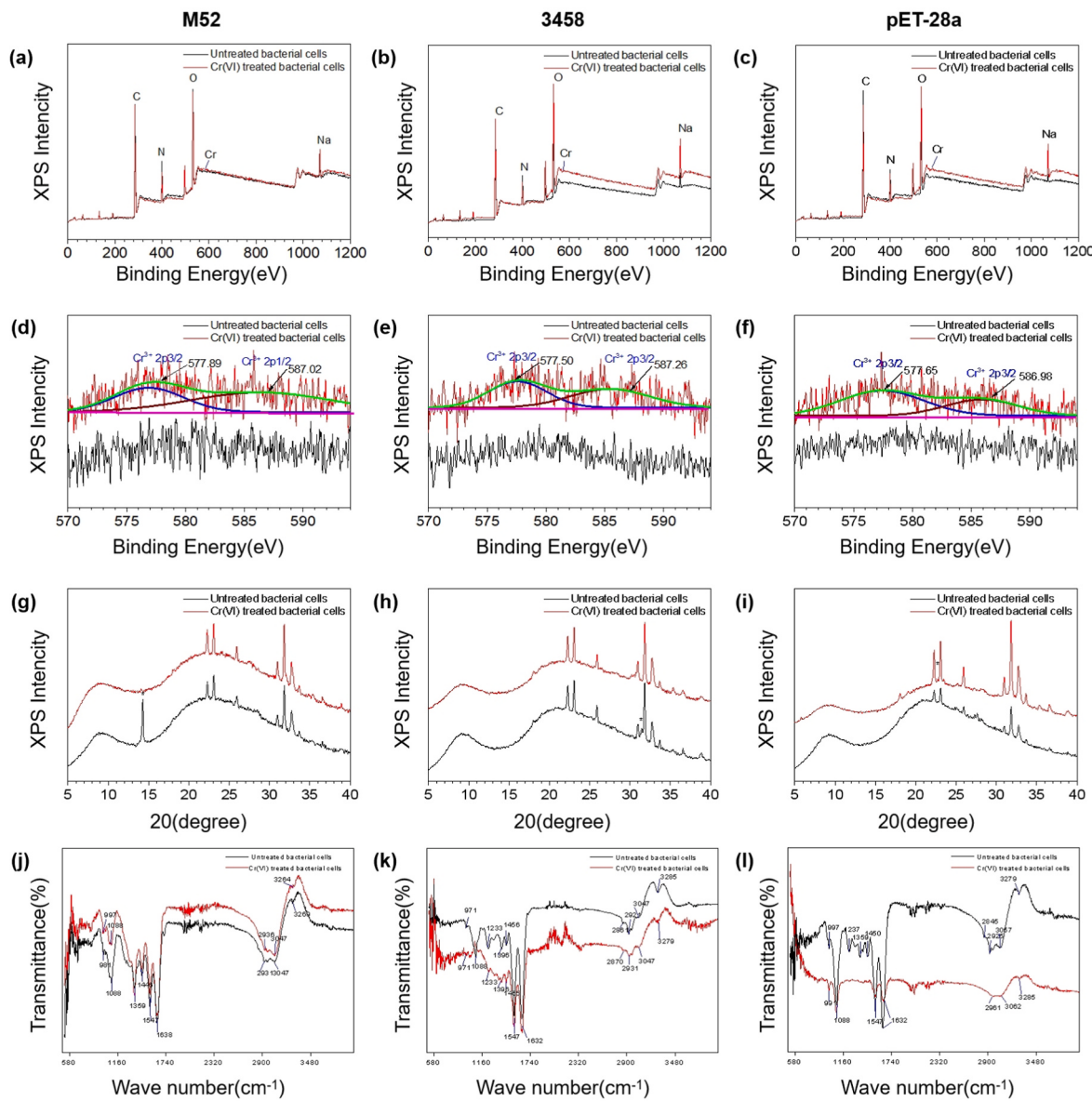


**Fig. 3.** The strains M52, recombinant strain 3458 and pET-28a of (a–f) XPS spectra, (g–i) XRD biomass spectrum, and (j–l) the FT-IR spectrum. Strains cultivated on LB medium with and without  $100 \text{ mg L}^{-1}$  Cr(VI) were used as the untreated bacterial cell and Cr(VI) treated bacterial cell, respectively. \*: The interaction between Cr (VI) and strain caused the diffraction peak to disappear, suggesting the change of strain structure.

### 3.5. Ecological safety of recombinant strain 3458 and its reduction system

#### 3.5.1. Effects on the sludge biological community

The community experiment of silt in water bodies was performed to evaluate alterations in the microbial community using high-throughput 16S rRNA sequencing, thereby examining the impact of recombinant strain 3458 as an introduced microorganism. Venn diagram analysis revealed that OTU numbers followed the order BC > PC > NC > 3458RS (Fig. 4a). Alpha diversity indices, including Observed species, ACE, and Chao1, serve as measures of community abundance, while Shannon and Simpson indices assess community diversity. Elevated values indicate greater community richness and diversity (Xiang et al., 2023; Yang et al., 2022). As listed in Table S7, BC group had the highest values for these indices, whereas the 3458RS group had the lowest, suggesting that changes in the cultural environment markedly affect community diversity and richness.

Comparisons of microbial community composition were conducted using beta diversity analysis. Both the multiple response permutation

procedure analysis (Table S8) and the principal coordinate analysis (PCoA) plot (Fig. 4b) revealed no significant differences in community structure among the groups ( $p > 0.05$ ). At the phylum level (Fig. 4c), *Proteobacteria*, *Firmicutes*, and *Bacteroidota* were the dominant phyla, which is consistent with most studies of the dominant phylum of soil communities contaminated with heavy metals (Yang et al., 2022). At the genus level (Fig. 4d), the dominance of *Acinetobacter*, *Pseudomonas*, and *Thiobacillus* in the 3458RS and PC groups indicates that chromium resistance/reduction genes possessed by these genera may facilitate Cr (VI) tolerance and removal (Ahmed, 2014; Malaviya and Singh, 2016).

FAPROTAX predicts the metabolic functions of microbial communities, particularly those involved in the cycling of carbon, nitrogen, phosphorus, and sulfur (Yang et al., 2022). Principal component analysis (PCA) of the FAPROTAX data revealed significant differences in the functional potential of microbial communities among the groups (Fig. 4e). Although previous beta diversity analysis showed no variation in community structure, functional PCA displayed complete separation, indicating that environmental stress, primarily from Cr(VI), modified the functional strategies of microorganisms without altering species

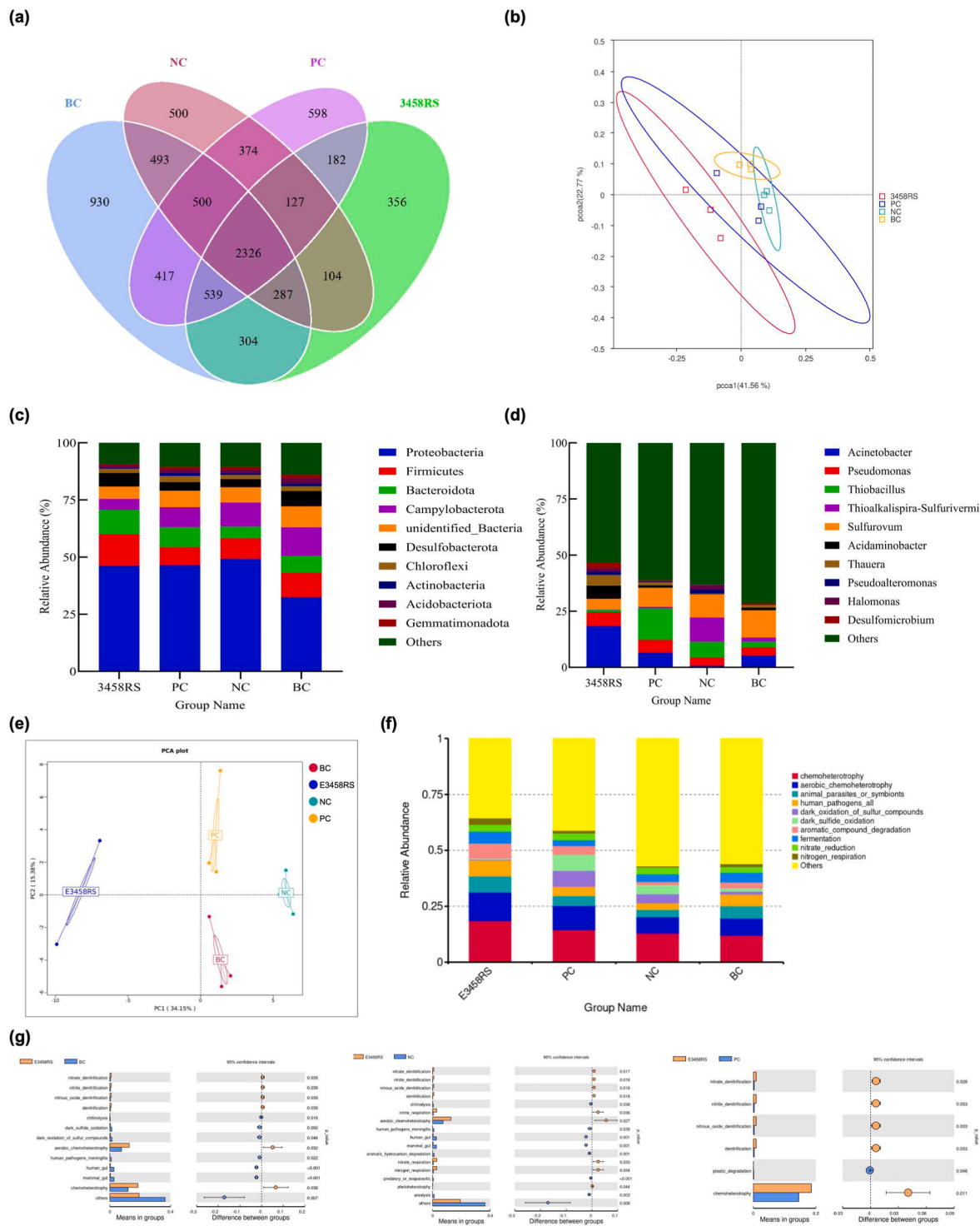


**Fig. 4.** Results of silt community analysis. (a) Venn diagram analysis between BC, NC, PC, and 3458RS groups. (b) PCoA analysis based on weighted unifrac distance. The coordinates indicate the principal components and the percentages indicate the contribution of the principal components to the sample difference. Species relative abundance histograms at (c) the phylum level and (d) the genus level. (e) PCA analysis based on functional abundance data between BC, NC, PC, and 3458RS groups. (f) Relative abundance bar chart according to the FAPROTAX database annotation. Relative abundance of the top-10 dominant functional groups. (g) t-test results for intergroup functional abundance data between BC, NC, PC, and 3458RS groups.

composition. Functional annotation relative abundance bar charts (Fig. 4f) and t-test results (Fig. 4g) demonstrated that, compared to each control group, the 3458RS group exhibited significantly increased functional activity in chemoheterotropy and nitrogen reduction processes (e.g., nitrate reduction, nitrate denitrification, and nitrite denitrification) ( $p < 0.05$ ). This increase may be due the upregulation of

functional gene expression in key microbial communities, such as denitrifying groups within the *Proteobacteria* phylum (Séneca et al., 2021), and chemolithotrophic bacteria like those in the *Firmicutes* phylum, which drive nitrogen-reducing enzyme activity through organic carbon metabolism (Liu et al., 2018). Additionally, Iqbal et al. (2024) reported significant differences in nitrogen-cycling functions among

wetland rhizosphere bacterial communities. Microorganisms may use soil carbon as their main energy source, which helps to remove nitrogen from the soil and is important for the nitrogen cycle (Liu et al., 2022).

Examining the alterations in alpha diversity metrics of strain 3458, the robust proliferation of the recombinant strain depleted significant nutrients and habitable space, markedly lowering oxygen levels and diminishing community diversity and richness. Nevertheless, under these unfavourable conditions, the *Proteobacteria* and *Actinobacteria* phyla, as dominant bacterial groups, had the potential for carbon and nitrogen cycling activated under Cr(VI) stress.

### 3.5.2. Growth inhibition of *Chlorella* sp

*Chlorella* is commonly employed as an experimental model for ecological assessments due to its responsiveness to environmental fluctuations, providing clear outcomes (Zhang et al., 2023). The normal proliferation of strains within the experimental system established a foundation for examining their impact on *Chlorella* growth (Fig. S4a). Over time, *Chlorella* populations in the NC group increased, attaining a maximum of  $2.00 \times 10^5$  mL<sup>-1</sup> on day 10, whereas growth in the other treatment groups was suppressed, varying within  $(8.50 \pm 1.67) \times 10^4$  mL<sup>-1</sup> (Fig. S4b). The growth of the NC group was significantly better than the other groups ( $p < 0.05$ ), but there was no significant difference ( $p > 0.05$ ), indicating that the effect of all experimental groups on *Chlorella* growth was essentially the same. Consistent with previous studies (Wenli et al., 2011), several conclusions were reached. First, a competitive interaction exists between the strain and *Chlorella*, leading to the cessation of *Chlorella* growth due to nutrient depletion. Second, the metabolic activity of the strains changed the environmental conditions during cultivation. For instance, excessive bacterial density inhibited algal growth (Yuting et al., 2015). Moreover, Xinyu et al. (2022) demonstrated that heavy metals are toxic to algae, impeding *Chlorella* photosynthesis.

## 3.6. Biosafety of recombinant strain 3458 and its reduction system

### 3.6.1. Evaluation of acute toxicity in mice

In practical applications, Cr(VI)-containing wastewater treated with bioremediation strains is discharged into natural water bodies, where the strain and RS are ingested by aquatic organisms such as fish and shrimp, ultimately entering the human body through the food chain. We evaluated the biosafety of strain 3458 and 3458RS using an acute oral toxicity test and observed no changes in clinical signs during the observation period. The body weight of mice steadily increased across all groups (Fig. S5), with no significant differences in weight gain rates between groups ( $p > 0.05$ ). Thus, we conclude that strain 3458 and 3458RS did not adversely affect physical growth or weight gain in the experimental mice.

### 3.6.2. Major organ coefficients and serum biochemical indexes

Considering the variety of exposure pathways and potential injuries, the liver, kidneys, and spleen were selected to calculate organ coefficients. As listed in Table S9, no significant differences were observed in organ coefficients of the liver and kidneys between all experimental and control groups ( $p > 0.05$ ), indicating that M52, 3458, and pET-28a and its reducing system did not affect mouse liver and kidney weights. The spleen coefficient was significantly smaller in all experimental groups compared to the NC and PC groups ( $p < 0.05$ ). However, inter-group differences were not statistically significant ( $p > 0.05$ ), likely because the experimental groups had a slightly higher body weight baseline than the controls. Combined with the relatively light spleen weight, this resulted in more pronounced fluctuations without clinical significance.

Serum biochemical indicators are crucial for assessing animal metabolism and organ function (Canh Pham et al., 2023), and these data are shown in Table S10. Compared to the NC group, the PC group exhibited higher AST and GLB, lower ALP liver function indicators ( $p <$

0.05), lower HDL-C and higher LDL-C lipid indicators ( $p < 0.05$ ), reduced Mg levels ( $p < 0.05$ ), and no changes in kidney function ( $p > 0.05$ ). Abnormal lipid metabolism is generally characterized by low HDL-C and high LDL-C levels (Wang et al., 2018; Wang et al., 2016), while elevated serum ALT and AST levels indicate acute hepatocellular injury (Lehmann-Werman et al., 2018). A study on the effects of Cr(VI) exposure on tilapia liver and kidneys demonstrated a significant increase in lipid content and serum ALT and AST levels in the Cr(VI)-treated group, attributed to enzyme leakage caused by liver injury (Mohamed et al., 2020). Although the Cr(VI) intake of mice in the PC group was less than 10 % LD<sub>50</sub>, the results indicated abnormal liver function and lipid levels.

TP serves as a crucial indicator for disease detection, with its immunoglobulin component GLB potentially linked to inflammation when both are elevated (Ping et al., 2015). Elevated levels of UA and urea signify abnormal renal metabolism (Weiner et al., 2015). Inorganic ions including Mg, Ca, and P, are essential electrolytes for maintaining homeostasis and acid-base balance (Ibrahim et al., 2022). Compared to the NC group, the M52, 3458, and pET-28a groups exhibited increased levels of ALT, AST, T-Bil, TP, GLB, UA, TG, LDL-C, and Ca, while HDL-C, Mg, and P levels decreased ( $p < 0.05$ ). Similarly, relative to the PC group, the MRS, 3458RS, and pET-28aRS groups showed elevated levels of ALT, AST, T-Bil, TP, UA, TG, LDL-C, and Ca, while urea, HDL-C, and P levels decreased ( $p < 0.05$ ). These results indicate liver damage, such as hepatitis, and abnormal lipid and electrolyte imbalances across all experimental groups.

Compared with their respective strains, the MRS, 3458RS, and pET-28aRS groups displayed an increase in ALT, AST, T-Bil, and UA indicators ( $p < 0.05$ ), whereas no significant changes were observed in blood lipid and inorganic salt ion indicators ( $p > 0.05$ ). This finding indicates that liver damage was more severe due to the presence of Cr (VI) in the reducing system, but lipid metabolism abnormalities were primarily caused by the strains. Based on the observed alterations in serum biochemical indices, we conclude that aside from the hepatic injury induced by Cr(VI) in the reducing system, M52, 3458, and pET-28a may impact liver function, lipid metabolism, and electrolyte balance in mice. However, the origin and severity of the toxicity warrant further investigation.

### 3.6.3. Analysis of liver tissue sections

As displayed in Fig. 5a, biopsies from the NC group exhibited no significant pathology, whereas mild congestion of the hepatic sinusoids was present in the PC and all experimental groups. Additionally, all experimental groups displayed cellular swelling and glass-like inclusions, which were more pronounced in the reducing systems compared to the strains. This may be attributed to the presence of Cr(VI) in the reducing system, which animal studies have demonstrated causes hepatocyte vacuolation, diffuse necrosis of the liver parenchyma, and inflammatory cell infiltrates (Tandon, 1982). Liver histopathology findings were consistent with the serum biochemical indices, but the underlying cause of the damage requires further analysis, including investigations into apoptosis and oxidative stress.

TUNEL staining showed the number of apoptotic hepatocytes was significantly increased in all experimental groups and the PC group compared to the NC group (Fig. 5b–c,  $p < 0.05$ ), while the number of apoptotic hepatocytes increased significantly in pET-28a and pET-28aRS compared to the PC group ( $p < 0.05$ ), ranked in severity as pET-28a > 3458 > M52.

### 3.6.4. Liver oxidative stress indicators and apoptotic protein assays

Oxidative stress serves as the pathophysiological foundation for multiple liver diseases (Li et al., 2015). SOD, an antioxidant metalloenzyme, and GSH-Px, a peroxidolytic enzyme, both function as anti-oxidants (Ighodaro and Akinloye, 2018). Conversely, MDA, an oxidative stress marker is product when free radicals attack body fat (Dashti et al., 2022; Gao et al., 2023). As listed in Table S11, MDA levels increased and

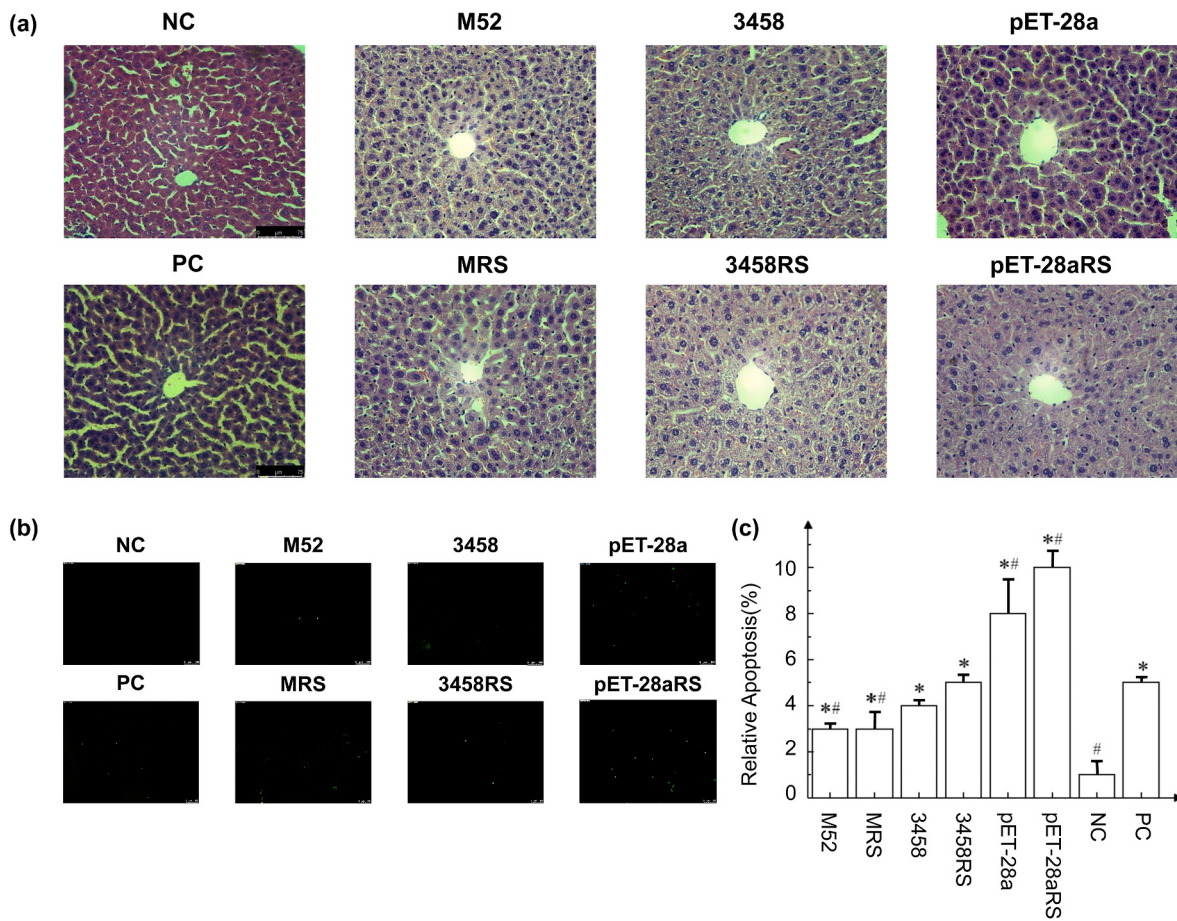


**Fig. 5.** Results of liver tissue section analyzes. (a) HE staining of liver biopsy of NC, PC, M52, MRS, 3458, 3458RS, pET-28a and pET-28aRS. TUNEL staining of liver biopsy of NC, PC, M52, MRS, 3458, 3458RS, pET-28a and pET-28aRS, involving (b) imaging and (c) quantification results. \*: Statistical difference compared with NC group ( $p < 0.05$ ); #: Statistical compared with PC group ( $p < 0.05$ ).

T-SOD levels declined in all experimental groups ( $p < 0.05$ ), but there was no significant differences were detected between groups ( $p > 0.05$ ). These results suggest that liver injury and disrupted lipid metabolism in M52, MRS, 3458, 3458RS, pET-28a, and pET-28aRS are likely due to increased oxidative stress in hepatocytes caused by excessive reactive oxygen species production.

Bcl-2 is an apoptosis-inhibiting protein that preserves mitochondrial integrity by antagonizing the proapoptotic Bax (Sun et al., 2019). The

Bax/Bcl-2 ratio is a crucial determinant of apoptosis induction: lower values indicate greater antiapoptotic capacity. Western blot results are shown in Fig. 6a. The Bax/Bcl-2 ratios for the M52, MRS, 3458, 3458RS, pET-28a, pET-28aRS, NC, and PC groups were 0.59, 0.96, 2.44, 2.07, 4.58, 1.35, 0.72, and 1.06, respectively. These results demonstrate that the antiapoptotic abilities of the strains follow the order: M52 > 3458 > pET-28a. pET-28a had the weakest antiapoptotic ability, so apoptosis was the most severe, consistent with the TUNEL staining results. In the

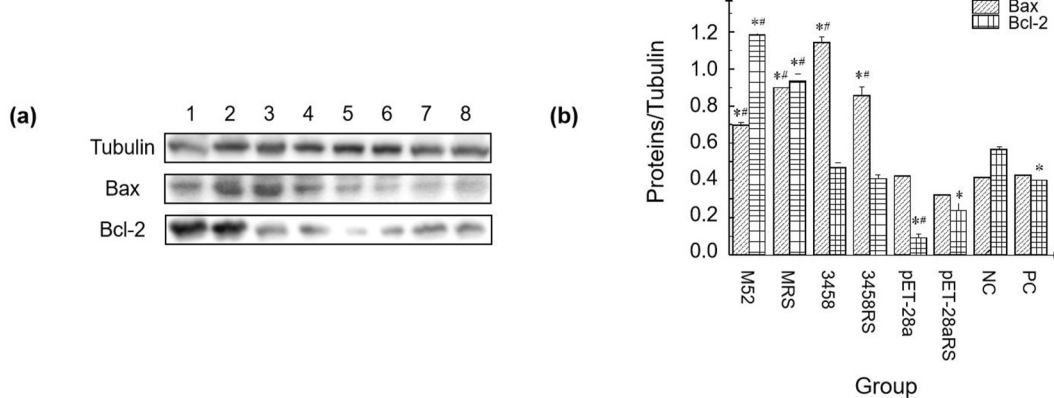


**Fig. 6.** Apoptosis-related protein expression and levels in liver tissue for each group. (a) Expression of tubulin, Bax, and Bcl-2 in M52 (1), MRS (2), 3458 (3), 3458RS (4), pET-28a (5), pET-28aRS (6), NC (7) and PC (8) groups. (b) Bax and Bcl-2 content after calibration with internal reference protein tubulin for each group. \*: Statistical difference compared with NC group ( $p < 0.05$ ); #: Statistical compared with 3458 group ( $p < 0.05$ ).

pET-28a group, Bcl-2 levels were significantly decreased (Fig. 6b,  $p < 0.05$ ) indicating that pET-28a may induce apoptosis by downregulating Bcl-2 protein expression.

Exposure to Cr(VI) is associated with liver injury involving oxidative stress and apoptosis (Su et al., 2024; Yang et al., 2020). Numerous animal models and cell line studies have demonstrated that oxidative stress, triggered by an increase in reactive oxygen species following Cr (VI) exposure, damages the lungs, liver, and kidneys (Chakraborty et al., 2022). The greater severity observed in liver tissue compared to other strains may be attributed to the reduction of Cr(VI) to Cr(III), which generates reactive oxygen species that harm cell membranes, proteins, and DNA (Flipkens et al., 2021). Lipopolysaccharide (LPS), a key component of gram-negative bacterial cell walls, comprises three-fourths of the *E. coli* cell wall and is also known as endotoxin. LPS primarily exerts its toxic effects by lysing and destroying bacteria and subsequently interacting with inflammatory factor receptors on target cells, such as TLR4 (Harper et al., 2011; Meszaros et al., 2016). Harper et al. (2011) administered LPS extracted from *E. coli* BL21 to CD-1 mice via oral gavage and observed no clinical signs or gross lesions. However, Wen et al. (2024) showed that the MDA content was significantly increased, the SOD content was significantly decreased, and the number of apoptotic cells was significantly increased in mouse lungs after LPS exposure. Zhao et al. (Zhao et al., 2014) treated A549 cells with LPS and observed a significant reduction in Bcl-2 protein expression compared to the control group, thereby confirming the role of Bcl-2 in LPS-induced apoptosis. Therefore, liver injury in mice treated with 3458 and pET-28a primarily stems from LPS's effect on cell walls. The recombinant strain 3458 mitigates some of these effects, though not entirely, likely because ChrA is a transport protein that alters cell wall composition.

Thus, strain 3458 demonstrates considerable repair potential, but concerns have been raised about its biosafety. A series of follow-up measures is recommended to address the safety risks associated with the recombinant strain in practical applications. First, constructing a biofilm reactor can physically isolate and restrict the dissemination of the recombinant strain, thereby reducing its potential risk to the environment and living organisms. Biofilms are microbial communities that adhere to solid surfaces for growth and reproduction. They not only protect bacteria from environmental stress but also enhance nutrient acquisition and increase resistance to antimicrobial agents (Das et al., 2024; Lago et al., 2024). Huang et al. (Huang et al., 2019) developed a *Bacillus subtilis* biofilm capable of degrading 2-hydroxyethyl terephthalate into the less toxic terephthalic acid. Second, given the characteristics of biofilm reactors, it is feasible to consider disinfecting the strains and recycling the resources. You et al. (2024) demonstrated that conventional chlorination and UV disinfection methods effectively inactivate pET-28a and recombinant strain 3458. Additionally, high-temperature treatment can deactivate the LPS present on the surface of *E. coli*, thereby preventing the initiation of inflammatory response. Furthermore, substituting the host strain with Gram-positive bacteria (e.g., *Bacillus subtilis*) or fungi (e.g., *Saccharomyces cerevisiae*) should be considered. These microorganisms can adsorb Cr(VI) and lack LPS on their cell surfaces, thereby circumventing LPS-related toxicity issues. These enhancements effectively mitigate health risks and further increase the utility of recombinant strains in managing heavy metal pollution.

#### 4. Conclusions

We constructed recombinant strain 3458, expressing a Cr(VI) removal gene. Compared to the original strain M52, recombinant strain 3458 exhibited comparable Cr(VI) resistance and removal capacity. Moreover, it demonstrated a broader range of applicability and capable of adsorbing the reduction products, facilitating metal recovery. This study also explored the safety of the strain. Recombinant strain 3458 affected the growth of *Chlorella* and the silt community, primarily

through competitive inhibition rather than toxicity. Animal safety studies suggest that recombinant strain 3458 causes liver damage and lipid abnormalities, mainly due to LPS on the *E. coli* BL21 surface, with the potential to induce hepatitis and even systemic inflammation. Therefore, when utilizing recombinant strain 3458 for chromium wastewater treatment, it is essential to implement additional measures, such as constructing a biofilm reactor or applying high temperatures to inactivate *E. coli* LPS to mitigate health risks associated with the direct release of the bioremediation strain into the environment. Furthermore, modifying the host to organisms like *Bacillus subtilis* or *Saccharomyces cerevisiae*, which can adsorb Cr(VI), can reduce the impact of LPS and promote Cr(VI) recycling, thereby enhancing the value of the recombinant strains.

#### CRediT authorship contribution statement

**Yeting Weng:** Writing – original draft, Visualization, Methodology, Investigation, Formal analysis, Conceptualization. **Qiuying An:** Writing – review & editing, Visualization, Methodology, Data curation. **Dongbei Guo:** Supervision, Resources, Project administration. **Ningjing Gan:** Visualization, Methodology, Data curation. **Weijie Zeng:** Visualization, Software. **Wanting You:** Writing – review & editing, Methodology, Investigation. **Zhangye Ma:** Validation, Investigation. **Jiayan Qi:** Validation, Investigation. **Zhiyu Zhang:** Visualization, Validation. **Lirong Zhang:** Visualization, Validation. **Mufeng Liang:** Validation, Methodology. **Hongyuan Zeng:** Validation, Methodology. **Xiaofen Zhang:** Supervision, Resources, Project administration. **Changsong Zhao:** Resources, Funding acquisition. **Ran Zhao:** Writing – review & editing, Supervision, Resources, Project administration, Methodology, Funding acquisition.

#### Declaration of competing interest

The authors declare that they have no known competing financial interests or personal relationships that could have appeared to influence the work reported in this paper.

#### Acknowledgments

This research was supported by the National Natural Science Foundation of China (No. 82473587, 81673129); Fujian Provincial Natural Science Foundation of China (No. 2024J01045); the Natural Science Foundation of Xiamen city (No. 3502Z20227178), the Xiamen University Open Project of High Level Public Health College (grant No. XMU-CMC202404), and Xiamen University Training Program of Innovation and Entrepreneurship for Undergraduates (No. S202410384472).

#### Appendix A. Supplementary data

Supplementary data to this article can be found online at <https://doi.org/10.1016/j.jenvman.2025.126653>.

#### Data availability

Data will be made available on request.

#### References

- Ahemad, M., 2014. Bacterial mechanisms for Cr(VI) resistance and reduction: an overview and recent advances. *Folia Microbiol.* 59 (4), 321–332. <https://doi.org/10.1007/s12223-014-0304-8>.
- Ahmad, S., Mfarrej, M.F.B., El-Esawi, M.A., Waseem, M., Alatawi, A., Nafees, M., Saleem, M.H., Rizwan, M., Yasmeen, T., Anayat, A., Ali, S., 2022. Chromium-resistant *Staphylococcus aureus* alleviates chromium toxicity by developing synergistic relationships with zinc oxide nanoparticles in wheat. *Ecotoxicol. Environ. Saf.* 230, 113142. <https://doi.org/10.1016/j.ecoenv.2021.113142>.
- Amanat, M., Shahid Ud Daula, A.F.M., Singh, R., 2023. Acute toxicity assessment of methanolic extract of *Zingiber roseum* (Roscoe.) rhizome in Swiss albino mice.

- Pharmacological Research - Modern Chinese Medicine 7, 100244. <https://doi.org/10.1016/j.jprmcm.2023.100244>.
- An, Q., Deng, S., Xu, J., Nan, H., Li, Z., Song, J.-L., 2020. Simultaneous reduction of nitrate and Cr(VI) by Pseudomonas aeruginosa strain G12 in wastewater. *Ecotoxicol. Environ. Saf.* 191, 110001. <https://doi.org/10.1016/j.ecoenv.2019.110001>.
- An, Q., Zhang, M., Guo, D., Wang, G., Xu, H., Fan, C., Li, J., Zhang, W., Li, Y., Chen, X., You, W., Zhao, R., 2022. Cr(VI) removal by recombinant Escherichia coli harboring the main functional genes of Sporosarcina saromensis M52. *Front. Microbiol.* 13.
- Aryal, M., 2024. Rhizomicrobiome dynamics: a promising path towards environmental contaminant mitigation through bioremediation. *J. Environ. Chem. Eng.* 12 (2), 112221. <https://doi.org/10.1016/j.jece.2024.112221>.
- Ayub, A., Wani, A.K., Malik, S.M., Ayub, M., Chopra, C., Singh, R., Malik, T., 2025. Harnessing microbes and plants for bioremediation of heavy metal contaminants: current paradigms and future perspectives. *Environ. Chall.*, 101220 <https://doi.org/10.1016/j.jenvc.2025.101220>.
- Berna, F., 2017. Fourier transform infrared spectroscopy (FTIR). In: Gilbert, A.S. (Ed.), *Encyclopedia of Geoarchaeology*. Dordrecht: Springer, Netherlands, pp. 285–286.
- Bharagava, R.N., Mishra, S., 2018. Hexavalent chromium reduction potential of sp isolated from common effluent treatment plant of tannery industries. *Ecotoxicol. Environ. Saf.* 147, 102–109. <https://doi.org/10.1016/j.ecoenv.2017.08.040>.
- Bhunia, A., Lahiri, D., Nag, M., Upadhye, V., Pandit, S., 2022. Bacterial biofilm mediated bioremediation of hexavalent chromium: a review. *Biocatal. Agric. Biotechnol.* 43, 102397. <https://doi.org/10.1016/j.bcab.2022.102397>.
- Boussouga, Y.-A., Okkali, T., Luxbacher, T., Schäfer, A.I., 2023. Chromium (III) and chromium (VI) removal and organic matter interaction with nanofiltration. *Sci. Total Environ.* 885, 163695. <https://doi.org/10.1016/j.scitotenv.2023.163695>.
- Canh Pham, E., Van, L.V., Nguyen, C.V., Duong, N.T.N., Le Thi, T.V., Truong, T.N., 2023. Acute and sub-acute toxicity evaluation of Merremia tridentata (L.) stem extract on mice. *Toxicicon* 227, 107093. <https://doi.org/10.1016/j.toxicon.2023.107093>.
- Chakraborty, R., Renu, K., Eladl, M.A., El-Sherbiny, M., Elsherbin, D.M.A., Mirza, A.K., Vellingiri, B., Iyer, M., Dey, A., Valsala Gopalakrishnan, A., 2022. Mechanism of chromium-induced toxicity in lungs, liver, and kidney and their ameliorative agents. *Biomed. Pharmacother.* 151, 113119. <https://doi.org/10.1016/j.biopha.2022.113119>.
- Chang, J., Deng, S., Liang, Y., Chen, J., 2019. Cr(VI) removal performance from aqueous solution by pseudomonas sp. strain DC-B3 isolated from mine soil: characterization of both Cr(VI) bioreduction and total Cr biosorption processes. *Environ. Sci. Pollut. Res. Int.* 26 (27), 28135–28145. <https://doi.org/10.1007/s11356-019-06017-w>.
- Chen, W., Zhou, T., Liu, Y., Luo, L., Ye, Y., Wei, L., Chen, J., Bian, Z., 2025. Genetically engineered bacteria expressing IL-34 alleviate experimental colitis by promoting tight junction protein expression in intestinal mucosal epithelial cells. *Mol. Immunol.* 178, 64–75. <https://doi.org/10.1016/j.molimm.2025.01.008>.
- Chrysochoou, M., Theologou, E., Bompoti, N., Dermatas, D., Panagiotakis, I., 2016. Occurrence, origin and transformation processes of geogenic chromium in soils and sediments. *Curr. Pollut. Rep.* 2 (4), 224–235. <https://doi.org/10.1007/s40726-016-0044-2>.
- Council, N.R., 2011. *Guide for the Care and Use of Laboratory Animals: Eighth Edition*. The National Academies Press, Washington, DC.
- Das, S., Pradhan, T., Panda, S.K., Behera, A.D., Kumar, S., Mallick, S., 2024. Bacterial biofilm-mediated environmental remediation: navigating strategies to attain sustainable development goals. *J. Environ. Manag.* 370, 122745. <https://doi.org/10.1016/j.jenvman.2024.122745>.
- Dashti, A., Shokrzaheh, M., Karimi, M., Habibi, E., 2022. Phytochemical identification, acute and subchronic oral toxicity assessments of hydroalcoholic extract of *Acropitilon repens* in BALB/c mice: a toxicological and mechanistic study. *Heliyon* 8 (2), e08940. <https://doi.org/10.1016/j.heliyon.2022.e08940>.
- Díaz-Pérez, C., Cervantes, C., Campos-García, J., Julián-Sánchez, A., Riveros-Rosas, H., 2007. Phylogenetic analysis of the chromate ion transporter (CHR) superfamily. *FEBS J.* 274 (23), 6215–6227. <https://doi.org/10.1111/j.1742-4658.2007.06141.x>.
- Flipkens, G., Blust, R., Town, R.M., 2021. Deriving nickel (Ni(II)) and chromium (Cr(III)) based environmentally safe olivine guidelines for coastal enhanced silicate weathering. *Environ. Sci. Technol.* 55 (18), 12362–12371. <https://doi.org/10.1021/acs.est.1c02974>.
- Gabr, R.M., Gad-Elrab, S.M.F., Abskharon, R.N.N., Hassan, S.H.A., Shoreit, A.A.M., 2009. Biosorption of hexavalent chromium using biofilm of *E. coli* supported on granulated activated carbon. *World J. Microbiol. Biotechnol.* 25 (10), 1695–1703. <https://doi.org/10.1007/s11274-009-0063-x>.
- Gao, C., Liu, C., Wei, Y., Wang, Q., Ni, X., Wu, S., Fang, Y., Hao, Z., 2023. The acute oral toxicity test of ethanol extract of salt-processed psoraleae fructus and its acute hepatotoxicity and nephrotoxicity risk assessment. *J. Ethnopharmacol.* 309, 116334. <https://doi.org/10.1016/j.jep.2023.116334>.
- Glandorf, D.C.M., 2019. Re-evaluation of biosafety questions on genetically modified biocontrol bacteria. *Eur. J. Plant Pathol.* 154 (1), 43–51. <https://doi.org/10.1007/s10658-018-1598-1>.
- González-González, R.B., Flores-Contreras, E.A., Parra-Saldívar, R., Iqbal, H.M.N., 2022. Bio-removal of emerging pollutants by advanced bioremediation techniques. *Environ. Res.* 214, 113936. <https://doi.org/10.1016/j.envrres.2022.113936>.
- Gu, R., Gao, J., Dong, L., Liu, Y., Li, X., Bai, Q., Jia, Y., Xiao, H., 2020. Chromium metabolism characteristics of coexpression of ChrA and ChrT gene. *Ecotoxicol. Environ. Saf.* 204, 111060. <https://doi.org/10.1016/j.ecoenv.2020.111060>.
- Harper, M.S., Carpenter, C., Klocke, D.J., Carlson, G., Davis, T., Delaney, B., 2011. *E. coli* lipopolysaccharide: acute oral toxicity study in mice. *Food Chem. Toxicol.* 49 (8), 1770–1772. <https://doi.org/10.1016/j.fct.2011.04.025>.
- Harutyunyan, V.S., 2022. XRD and combined SEM-EDS analysis of long-term hydration products of ye'elimité. *Mater. Chem. Phys.* 276. <https://doi.org/10.1016/j.matchemphys.2021.125373>.
- Hou, D., O'Connor, D., Igavathana, A.D., Alessi, D.S., Luo, J., Tsang, D.C.W., Sparks, D.L., Yamauchi, Y., Rinklebe, J., Ok, Y.S., 2020. Metal contamination and bioremediation of agricultural soils for food safety and sustainability. *Nat. Rev. Earth Environ.* 1 (7), 366–381. <https://doi.org/10.1038/s43017-020-0061-y>.
- Huang, J., Liu, S., Zhang, C., Wang, X., Pu, J., Ba, F., Xue, S., Ye, H., Zhao, T., Li, K., Wang, Y., Zhang, J., Wang, L., Fan, C., Lu, T.K., Zhong, C., 2019. Programmable and printable *Bacillus subtilis* biofilms as engineered living materials. *Nat. Chem. Biol.* 15 (1), 34–41. <https://doi.org/10.1038/s41589-018-0169-2>.
- Huang, W., Chen, H., Jia, M., Li, Q., Chen, M., Guo, X., 2024. Genomic and proteomic analyses reveal the reduction mechanism of hexavalent chromium by the culturing supernatant of strain *Pediococcus acidilactici* 13-7. *J. Hazard Mater.* 477, 135161. <https://doi.org/10.1016/j.jhazmat.2024.135161>.
- Ibrahim, S.L., Alzubaidi, Z.F., Al-Maamory, F.A.D., 2022. Electrolyte disturbances in a sample of hospitalized patients from Iraq. *J. Med. Life* 15 (9), 1129–1135. <https://doi.org/10.2512/jml-2022-0039>.
- Ighodaro, O.M., Akinloye, O.A., 2018. First line defence antioxidants-superoxide dismutase (SOD), catalase (CAT) and glutathione peroxidase (GPX): their fundamental role in the entire antioxidant defence grid. *Alexandria Journal of Medicine* 54 (4), 287–293. <https://doi.org/10.1016/j.ajme.2017.09.001>.
- Iqbal, A., Maqsood Ur Rehman, M., Sajjad, W., Degen, A.A., Rafiq, M., Jiahuan, N., Khan, S., Shang, Z., 2024. Patterns of bacterial communities in the rhizosphere and rhizoplane of alpine wet meadows. *Environ. Res.* 241, 117672. <https://doi.org/10.1016/j.envres.2023.117672>.
- Karthik, C., Barathi, S., Pugazhendhi, A., Ramkumar, V.S., Thi, N.B.D., Arulselvi, P.I., 2017. Evaluation of Cr(VI) reduction mechanism and removal by *Cellulosimicrobium funkei* strain AR8, a novel haloalkaliphilic bacterium. *J. Hazard Mater.* 333, 42–53. <https://doi.org/10.1016/j.jhazmat.2017.03.037>.
- Ke, C., Zhao, C., Rensing, C., Yang, S., Zhang, Y., 2018. Characterization of recombinant *E. coli* expressing arsR from *Rhodopseudomonas palustris* CGA009 that displays highly selective arsenic adsorption. *Appl. Microbiol. Biotechnol.* 102 (14), 6247–6255. <https://doi.org/10.1007/s00253-018-9080-8>.
- Krishna, D.N.G., Philip, J., 2022. Review on surface-characterization applications of X-ray photoelectron spectroscopy (XPS): recent developments and challenges. *Appl. Surf. Sci. Adv.* 12, 100332. <https://doi.org/10.1016/j.apsadv.2022.100332>.
- Lago, A., Rocha, V., Barros, O., Silva, B., Tavares, T., 2024. Bacterial biofilm attachment to sustainable carriers as a clean-up strategy for wastewater treatment: a review. *J. Water Proc. Eng.* 63, 105368. <https://doi.org/10.1016/j.jwpe.2024.105368>.
- Layek, M., Khatun, N., Karmakar, P., Kundu, S., Mitra, M., Karmakar, K., mondal, S., Bhattacharai, A., Saha, B., 2023. Toxicity of hexavalent chromium: review. In: Kumar, N., Walther, C., Gupta, D.K. (Eds.), *Chromium in Plants and Environment*. Springer Nature Switzerland, Cham, pp. 191–215.
- Lehmann-Werman, R., Magenheim, J., Moss, J., Neiman, D., Abraham, O., Piyanzin, S., Zemmour, H., Fox, I., Dor, T., Grompe, M., Landesberg, G., Loza, B.L., Shaked, A., Olthoff, K., Glaser, B., Shemer, R., Dor, Y., 2018. Monitoring liver damage using hepatocyte-specific methylation markers in cell-free circulating DNA. *JCI Insight* 3 (12). <https://doi.org/10.1172/jci.insight.120687>.
- Lei, D., Zhang, L., Yan, H., Liu, Y., Peng, X., Xiao, W., Bi, Q., Xue, J., Wang, Y., 2023. Simultaneous removal of Arsenic(III) and Chromium(VI) over ZnFe2O4 {100}/{111} Z-scheme photocatalyst: Facet-dependent active site and overlooked As(III)/Cr(VI) complex. *J. Clean. Prod.* 383, 135493. <https://doi.org/10.1016/j.jclepro.2022.135493>.
- Li, J., Tang, C., Zhang, M., Fan, C., Guo, D., An, Q., Wang, G., Xu, H., Li, Y., Zhang, W., Chen, X., Zhao, R., 2021. Exploring the Cr(VI) removal mechanism of *Sporosarcina saremensis* M52 from a genomic perspective. *Ecotoxicol. Environ. Saf.* 225, 112767. <https://doi.org/10.1016/j.ecoenv.2021.112767>.
- Li, Q., Zhang, X., Qin, J., Liao, Q., Si, M., Yang, Z., Yang, W., Lin, Z., 2025. Unraveling the critical role of accelerated extracellular electron transfer in the microbial galvanic effect driving mineral-bound Cr(VI) effective release and bioreduction. *Chem. Eng. J.* 519, 165480. <https://doi.org/10.1016/j.cej.2025.165480>.
- Li, S., Tan, H.Y., Wang, N., Zhang, Z.J., Lao, L., Wong, C.W., Feng, Y., 2015. The role of oxidative stress and antioxidants in liver diseases. *Int. J. Mol. Sci.* 16 (11), 26087–26124. <https://doi.org/10.3390/ijms161125942>.
- Li, W., Liu, Y., Zheng, X., Han, J., Shi, A., Wong, C.C., Wang, R., Jing, X., Li, Y., Fan, S., Zhang, C., Chen, Y., Guo, G., Yu, J., She, J., 2024. Rewiring tryptophan metabolism via programmable probiotic integrated by dual-layered microcapsule protects against inflammatory bowel disease in mice. *ACS Nano*. <https://doi.org/10.1021/acsnano.4c12801>.
- Liu, H., Wang, Y., Zhang, H., Huang, G., Yang, Q., Wang, Y., 2019. Synchronous detoxification and reduction treatment of tannery sludge using Cr (VI) resistant bacterial strains. *Sci. Total Environ.* 687, 34–40. <https://doi.org/10.1016/j.scitotenv.2019.06.093>.
- Liu, J.P., Fan, Y.P., Liu, X.Z., Wang, J.X., 2018. Communities and diversities of bacteria and archaea in arctic seawater. *Evol. Ecol. Res.* 19, 407–421.
- Liu, Y., Guo, Z., Zhang, P., Du, J., Gao, P., Zhang, Z., 2022. Diversity and structure of vegetation rhizosphere bacterial community in various habitats of liaohekou coastal wetlands. *Sustainability* 14 (24). <https://doi.org/10.3390/su142416396>.
- Long, D., Tang, X., Cai, K., Chen, G., Chen, L., Duan, D., Zhu, J., Chen, Y., 2013. Cr(VI) reduction by a potent novel alkaliphilic halotolerant strain *Pseudochrobactrum saccharolyticum* LY10. *J. Hazard Mater.* 256–257, 24–32. <https://doi.org/10.1016/j.jhazmat.2013.04.020>.
- Ly, N.H., Barceló, D., Vasseghian, Y., Choo, J., Joo, S.-W., 2024. Sustainable bioremediation technologies for algal toxins and their ecological significance. *Environ. Pollut.* 341, 122878. <https://doi.org/10.1016/j.envpol.2023.122878>.
- Malaviya, P., Singh, A., 2016. Bioremediation of chromium solutions and chromium containing wastewaters. *Crit. Rev. Microbiol.* 42 (4), 607–633. <https://doi.org/10.3109/1040841X.2014.974501>.

- Maqsood, Q., Sumrin, A., Waseem, R., Hussain, M., Imtiaz, M., Hussain, N., 2023. Bioengineered microbial strains for detoxification of toxic environmental pollutants. Environ. Res. 227, 115665. <https://doi.org/10.1016/j.envres.2023.115665>.
- Mertes, V., Saragliadis, A., Mascherin, E., Tysvær, E.-B., Roos, N., Linke, D., Winther-Larsen, H.C., 2024. Recombinant expression of *Yersinia ruckeri* outer membrane proteins in *Escherichia coli* extracellular vesicles. Protein Expr. Purif. 215, 106409. <https://doi.org/10.1016/j.pep.2023.106409>.
- Meszaros, A.V., Weidinger, A., Dorighello, G., Boros, M., Redl, H., Kozlov, A.V., 2016. 108 - the impact of inflammatory cytokines on liver damage caused by elevated generation of mitochondrial reactive oxygen species. Free Radic. Biol. Med. 100, S57. <https://doi.org/10.1016/j.freeradbiomed.2016.10.149>.
- Metcalfe, G.D., Sargent, F., Hippler, M., 2022. Hydrogen production in the presence of oxygen by *Escherichia coli* K-12. Microbiology (Read.) 168 (3). <https://doi.org/10.1099/mic.0.001167>.
- Mohamed, A.A.-R., El-Houseiny, W., El-Murr, A.E., Ebraheim, L.L.M., Ahmed, A.I., El-Hakim, Y.M.A., 2020. Effect of hexavalent chromium exposure on the liver and kidney tissues related the expression of CYP450 and GST genes of Oreochromis niloticus fish: role of curcumin supplemented diet. Ecotoxicol. Environ. Saf. 188, 109890. <https://doi.org/10.1016/j.ecoenv.2019.109890>.
- Mohamed, M.S.M., El-Arabi, N.I., El-Hussein, A., El-Matty, S.A., Abdelhadi, A.A., 2020. Reduction of chromium-VI by chromium-resistant *Escherichia coli* FACU: a prospective bacterium for bioremediation. Folia Microbiol. 65 (4), 687–696. <https://doi.org/10.1007/s12223-020-00771-y>.
- Pandey, A., Dalal, S., Dutta, S., Dixit, A., 2021. Structural characterization of polycrystalline thin films by X-ray diffraction techniques. J. Mater. Sci. Mater. Electron. 32 (2), 1341–1368. <https://doi.org/10.1007/s10854-020-04998-w>.
- Pimentel, B.E., Moreno-Sánchez, R., Cervantes, C., 2002. Efflux of chromate by *Pseudomonas aeruginosa* cells expressing the ChrA protein. FEMS (Fed. Eur. Microbiol. Soc.) Microbiol. Lett. 212 (2), 249–254. [https://doi.org/10.1016/S0378-1097\(02\)00755-3](https://doi.org/10.1016/S0378-1097(02)00755-3).
- Ping, L., Guang-fu, D., Xiao-quan, G., Jun, K., Caiying, Z., Huabin, C., Guoliang, H.J.P.V. J., 2015. Clinicopathology of Gout in Growing Layers Induced by Avian Nephrotrophic Strains of Infectious Bronchitis Virus, vol. 35, pp. 345–349.
- Qi, T., Zhang, S., Zhang, J., Li, T., Xing, L., Fang, Z., An, S., Xu, Z., Xiao, H., Wang, L., 2023. In situ reconstruction of active catalysis sites triggered by chromium immobilization for sulfite oxidation. Environ. Sci. Technol. 57 (9), 3905–3916. <https://doi.org/10.1012/est.2c09606>.
- Qiu, Y.-Y., Xia, J., Guo, J., Gong, X., Zhang, L., Jiang, F., 2024. Groundwater chromate removal by autotrophic sulfur disproportionation. Environ. Sci. Ecotechnol. 21, 100399. <https://doi.org/10.1016/j.est.2024.100399>.
- Qurbani, K., Khadir, K., Sidiq, A., Hamzah, H., Hussein, S., Hamad, Z., Abdulla, R., Abdulla, B., Azizi, Z., 2022. Aeromonas sobria as a potential candidate for bioremediation of heavy metal from contaminated environments. Sci. Rep. 12 (1), 21235. <https://doi.org/10.1038/s41598-022-25781-3>.
- Raturi, G., Chaudhary, A., Rana, V., Mandlik, R., Sharma, Y., Barvkar, V., Salvi, P., Tripathi, D.K., Kaur, J., Deshmukh, R., Dhar, H., 2023. Microbial remediation and plant-microbe interaction under arsenic pollution. Sci. Total Environ. 864, 160972. <https://doi.org/10.1016/j.scitotenv.2022.160972>.
- Rincon, S.M., Beyenal, H., Romero, H.M., 2024. A response surface methodology study for *Chlorella vulgaris* mixotrophic culture optimization. Microorganisms 12 (2). <https://doi.org/10.3390/microorganisms12020379>.
- Samuel, J., Paul, M.L., Ravishankar, H., Mathur, A., Saha, D.P., Natarajan, C., Mukherjee, A., 2013. The differential stress response of adapted chromite mine isolates *Bacillus subtilis* and *Escherichia coli* and its impact on bioremediation potential. Biodegradation 24 (6), 829–842. <https://doi.org/10.1007/s10532-013-9631-8>.
- Séneca, J., Söllinger, A., Herbold, C.W., Pjevac, P., Prommer, J., Verbruggen, E., Sigurdsson, B.D., Peñuelas, J., Janssens, I.A., Urich, T., Tveit, A.T., Richter, A., 2021. Increased microbial expression of organic nitrogen cycling genes in long-term warmed grassland soils. ISME Communications 1 (1), 69. <https://doi.org/10.1038/s43705-021-00073-5>.
- Shahid, M., Shamshad, S., Rafiq, M., Khalid, S., Bibi, I., Niazi, N.K., Dumat, C., Rashid, M. I., 2017. Chromium speciation, bioavailability, uptake, toxicity and detoxification in soil-plant system: a review. Chemosphere 178, 513–533. <https://doi.org/10.1016/j.chemosphere.2017.03.074>.
- Simas, R.G., Pessoa Junior, A., Long, P.F., 2023. Mechanistic aspects of IPTG (isopropylthio- $\beta$ -galactoside) transport across the cytoplasmic membrane of *Escherichia coli* - a rate limiting step in the induction of recombinant protein expression. J. Ind. Microbiol. Biotechnol. 50 (1). <https://doi.org/10.1093/jimb/kuad034>.
- Stewart, D.I., Vasconcelos, E.J.R., Burke, I.T., Baker, A., 2024. Metagenomes from microbial populations beneath a chromium waste tip give insight into the mechanism of Cr (VI) reduction. Sci. Total Environ. 931, 172507. <https://doi.org/10.1016/j.scitotenv.2024.172507>.
- Su, Z., Zhang, Y., Hong, S., Zhang, Q., Xu, J., Hu, G., Zhu, X., Yuan, F., Yu, S., Wang, T., Jia, G., 2024. Relationships between blood chromium exposure and liver injury: exploring the mediating role of systemic inflammation in a chromate-exposed population. J. Environ. Sci. 143, 224–234. <https://doi.org/10.1016/j.jes.2023.08.014>.
- Sun, T., Liu, H., Cheng, Y., Yan, L., Krittawong, C., Li, S., Qian, W., Su, W., Chen, X., Hou, X., Zhang, H., 2019. 2,3,5,4'-Tetrahydroxystilbene-2-O- $\beta$ -d-glucoside eliminates ischemia/reperfusion injury-induced H9c2 cardiomyocytes apoptosis involving in Bcl-2, bax, caspase-3, and akt activation. J. Cell. Biochem. 120 (7), 10972–10977. <https://doi.org/10.1002/jcb.27949>.
- Tan, C., Liu, H., 2023. Inhibition of hexavalent chromium release from drinking water distribution systems: effects of water chemistry-based corrosion control strategies. Environ. Sci. Technol. 57 (47), 18433–18442. <https://doi.org/10.1021/acs.est.2c05324>.
- Tan, H., Wang, C., Zeng, G., Luo, Y., Li, H., Xu, H., 2020. Bioreduction and biosorption of Cr(VI) by a novel bacillus sp. CRB-1 strain. J. Hazard Mater. 386, 121628. <https://doi.org/10.1016/j.jhazmat.2019.121628>.
- Tandon, S.K., 1982. Chapter 9 - organ toxicity of chromium in animals. In: LangÅRD, S. (Ed.), Biological and Environmental Aspects of Chromium. Elsevier, Amsterdam, pp. 209–220.
- Thatoi, H., Das, S., Mishra, J., Rath, B.P., Das, N., 2014. Bacterial chromate reductase, a potential enzyme for bioremediation of hexavalent chromium: a review. J. Environ. Manag. 146, 383–399. <https://doi.org/10.1016/j.jenvman.2014.07.014>.
- Wang, C., Kong, L., Yang, Y., Wei, Y., Zhu, W., Su, R., Lin, L., Yang, H., 2018. Recommended reference values for serum lipids during early and middle pregnancy: a retrospective study from China. Lipids Health Dis. 17 (1), 246. <https://doi.org/10.1186/s12944-018-0885-3>.
- Wang, J., Yu, W., Xu, J., Feng, L., Yang, H., Liu, X., 2016. [study on the prevalence of lipid metabolism disorders and quantitative analysis of apolipoproteins in T2DM patients]. Wei Sheng Yan Jiu 45 (4), 587–592.
- Weiner, I.D., Mitch, W.E., Sands, J.M., 2015. Urea and ammonia metabolism and the control of renal nitrogen excretion. Clin. J. Am. Soc. Nephrol. 10 (8), 1444–1458. <https://doi.org/10.2314/cjn.10311013>.
- Wen, H., Miao, W., Liu, B., Chen, S., Zhang, J.-S., Chen, C., Quan, M.-Y., 2024. SPAUTIN-1 alleviates LPS-Induced acute lung injury by inhibiting NF- $\kappa$ B pathway in neutrophils. Int. Immunopharmacol. 130, 111741. <https://doi.org/10.1016/j.intimp.2024.111741>.
- Wenli, Z., Hui, X., Xiuting, Q., Jingfeng, S., Kezhi, X., Xuexi, T., 2011. Quorum sensing of an associated heterotrophic Bacteria-Z-QS01 with *Chlorella Vulgaris* and response to enhanced UV- radiation. 北京理工大学学报 31 (1), 109–112. <https://doi.org/10.15918/j.tbit001-0645.2011.01.007>.
- Wu, M., Li, Y., Li, J., Wang, Y., Xu, H., Zhao, Y., 2019. Bioreduction of hexavalent chromium using a novel strain CRB-7 immobilized on multiple materials. J. Hazard Mater. 368, 412–420. <https://doi.org/10.1016/j.jhazmat.2019.01.059>.
- Xia, S.P., Song, Z.L., Jeyakumar, P., Shaheen, S.M., Rinklebe, J., Ok, Y.S., Bolan, N., Wang, H.L., 2019. A critical review on bioremediation technologies for Cr(VI)-contaminated soils and wastewater. Crit. Rev. Environ. Sci. Technol. 49 (12), 1027–1078. <https://doi.org/10.1080/10643389.2018.1564526>.
- Xiang, Y., Liu, Y., Niazi, N.K., Bolan, N., Zhao, L., Zhang, S., Xue, J., Yao, B., Li, Y., 2023. Biochar addition increased soil bacterial diversity and richness: Large-scale evidence of field experiments. Sci. Total Environ. 893, 164961. <https://doi.org/10.1016/j.scitotenv.2023.164961>.
- Xiao, B., Jia, J., Wang, W., Zhang, B., Ming, H., Ma, S., Kang, Y., Zhao, M., 2023. A review on magnetic biochar for the removal of heavy metals from contaminated soils: preparation, application, and microbial response. Journal of Hazardous Materials Advances 10, 100254. <https://doi.org/10.1016/j.hazadv.2023.100254>.
- Xinyu, Q., Jian, L., Xiaoxi, Y., Yiqin, W., Yao, Z., Wei, W., 2022. Aquatic environmental toxicology of *Chlorella pyrenoidosa* chick :Research progress and application prospect. 农学学报 12 (2), 65–72.
- Yang, M., Zhang, X., Sun, Y., 2024. Remediation of Cr(VI) polluted groundwater using zero-valent iron composites: preparation, modification, mechanisms, and environmental implications. Molecules 29 (23). <https://doi.org/10.3390/molecules29235697>.
- Yang, N., Li, X., Liu, D., Zhang, Y., Chen, Y., Wang, B., Hua, J., Zhang, J., Peng, S., Ge, Z., Li, J., Ruan, H., Mao, L., 2022. Diversity patterns and drivers of soil bacterial and fungal communities along elevational gradients in the Southern Himalayas, China. Appl. Soil Ecol. 178, 104563. <https://doi.org/10.1016/j.apsoil.2022.104563>.
- Yang, Q., Han, B., Xue, J., Lv, Y., Li, S., Liu, Y., Wu, P., Wang, X., Zhang, Z., 2020. Hexavalent chromium induces mitochondrial dynamics disorder in rat liver by inhibiting AMPK/PGC-1 $\alpha$  signaling pathway. Environ. Pollut. 265, 114855. <https://doi.org/10.1016/j.envpol.2020.114855>.
- Yang, Y., Zhang, J., Dong, S., Li, M., Yang, P., Meng, H., Xiao, J., 2024. Sustainable Cr (VI) reduction in a membrane-less TPBC-MPC driven by solid watermelon rind. J. Environ. Manag. 370, 122637. <https://doi.org/10.1016/j.jenvman.2024.122637>.
- Yang, Z.-N., Liu, Z.-S., Wang, K.-H., Liang, Z.-L., Abdugheni, R., Huang, Y., Wang, R.-H., Ma, H.-L., Wang, X.-K., Yang, M.-L., Zhang, B.-G., Li, D.-F., Jiang, C.-Y., Corvini, P.F., X., Liu, S.-J., 2022. Soil microbiomes divergently respond to heavy metals and polycyclic aromatic hydrocarbons in contaminated industrial sites. Environ. Sci. Ecotechnol. 10, 100169. <https://doi.org/10.1016/j.est.2022.100169>.
- Yang, Z., Peng, C., Cao, H., Song, J., Gong, B., Li, L., Wang, L., He, Y., Liang, M., Lin, J., Lu, L., 2022. Microbial functional assemblages predicted by the FAPROTAX analysis are impacted by physicochemical properties, but C, N and S cycling genes are not in mangrove soil in the Beibu Gulf, China. Ecol. Indic. 139, 108887. <https://doi.org/10.1016/j.ecolind.2022.108887>.
- You, W., An, Q., Guo, D., Huang, Z., Guo, L., Chen, Z., Xu, H., Wang, G., Weng, Y., Ma, Z., Chen, X., Hong, F., Zhao, R., 2024. Exploration of risk analysis and elimination methods for a Cr(VI)-removal recombinant strain through a biosafety assessment in mice. Sci. Total Environ. 912, 168743. <https://doi.org/10.1016/j.jest.2023.168743>.
- Yuting, Z., Bipeng, Y., Fei, Y., Yibin, S., Jiayun, S., 2015. Experimental Study on the effect of flow on the growth of *Microcystis aeruginosa*. 环境科学与技术 38 (11), 120–124.
- Zhang, K., Shi, Y., Xu, P., Huang, C., Zhou, C., Liu, P., Hu, R., Zhuang, Y., Li, G., Hu, G., Guo, X., 2021. Cloning and prokaryotic expression of the chicken liver kinase B1 (LKB1) and its localization in liver, heart and hypothalamus. Int. J. Biol. Macromol. 169, 513–520. <https://doi.org/10.1016/j.ijbiomac.2020.12.195>.
- Zhang, L., Zheng, X., Liu, X., Li, J., Li, Y., Wang, Z., Zheng, N., Wang, X., Fan, Z., 2023. Toxic effects of three perfluorinated or polyfluorinated compounds (PFCs) on two

- strains of freshwater algae: implications for ecological risk assessments. *J. Environ. Sci.* 131, 48–58. <https://doi.org/10.1016/j.jes.2022.10.042>.
- Zhao, J., Li, X., Zou, M., He, J., Han, Y., Wu, D., Yang, H., Wu, J., 2014. miR-135a inhibition protects A549 cells from LPS-induced apoptosis by targeting Bcl-2. *Biochem. Biophys. Res. Commun.* 452 (4), 951–957. <https://doi.org/10.1016/j.bbrc.2014.09.025>.
- Zhao, R., Wang, B., Cai, Q.T., Li, X.X., Liu, M., Hu, D., Guo, D.B., Wang, J., Fan, C., 2016. Bioremediation of hexavalent chromium pollution by *Sporosarcina saromensis* M52 isolated from offshore sediments in Xiamen, China. *Biomed. Environ. Sci.* 29 (2), 127–136. <https://doi.org/10.3967/bes2016.014>.
- Zhao, Y., Moore, O.W., Xiao, K.-Q., Otero-Fariña, A., Banwart, S.A., Wu, F.-C., Peacock, C.L., 2023. Behavior and fate of chromium and carbon during Fe(II)-Induced transformation of ferrihydrite organominerals. *Environ. Sci. Technol.* 57 (45), 17501–17510. <https://doi.org/10.1021/acs.est.3c05487>.